Optics Communications 282 (2009) 2212–2216

Contents lists available at ScienceDirect

Optics Communications

journal homepage: www.elsevier.com/locate/optcom

An intuitive picture of the physics underlying optical ranging using frequency shifted feedback lasers seeded by a phase-modulated field

L.P. Yatsenko [a], B.W. Shore [b,*], K. Bergmann [c]

[a] Institute of Physics, National Academy of Sciences of Ukraine Prospect, Nauki 46, Kiev-39, 03650, Ukraine
[b] 618 Escondido Circle, Livermore, CA 94550, USA
[c] Department of Physics and OPTIMAS Research Center at the Technical University, Kaiserslautern, 67653 Kaiserslautern, Germany

EXHIBIT C

ARTICLE INFO

Article history:
Received 24 November 2008
Accepted 16 February 2009

PACS:
42.30.–d
42.55.–f
42.60.Da
42.62.Eh

ABSTRACT

Frequency shifted feedback (FSF) lasers have been demonstrated to have interesting and useful features when used for optical ranging. The use of a phase-modulated seed to the FSF laser dramatically improves the signal-to-noise ratio, enabling distance measurements with the accuracy expected of optical interferometry. We present here an intuitively accessible description of the physics that underlies this dramatic enhancement of optical ranging signals. Unlike a free-running FSF laser, each one of the many equidistant frequency components of the seeded FSF laser spectrum (typically $>10^4$) has a definite amplitude, and a phase which varies with component number and modulation frequency Ω of the seed radiation. Suitable adjustment of Ω gives all components a common phase; the resulting constructive interference enhances the signal by orders of magnitude.

1. Introduction

Many optical ranging technologies make use of interference between two ray paths, one of known distance and the other to a target object, to measure distances with subwavelength accuracy. Lasers have served well as the radiation sources for optical ranging. In particular, frequency shifted feedback (FSF) lasers have been proposed and demonstrated [1–7]; their properties offer potential advantages over other laser-based techniques for ranging [8–13].

In recent papers [10,11,13] we have proposed and demonstrated the use of a FSF laser whose seed frequency is phase modulated. This easily implemented modification improves the signal-to-noise ratio by many orders of magnitude and thus overcomes some recognized problems. Although the mathematics has been presented in detail [10], and experimental demonstrations have been published [11,13], the mathematical formalism has provided no intuitive picture of the role of phase modulation.

We here offer a very simple presentation of the principles involved in the phase-modulated FSF laser and its use for optical ranging. To explain the technology we first review the basic operation of a Michelson interferometer, because this forms the heart of the ranging measurement. We start by pointing out, as is well known, how classical interferometry with monochromatic light has an intrinsic ambiguity in measuring lengths: these are determined only within a multiple of the optical wavelength. One technique for overcoming this limitation is the use of phase-modulated light as interferometer input, but this technique has limitations that we mention.

Having presented this background, we discuss how a phase-modulated FSF laser, being the superposition of a very large number (typically more than 10^4) of mutually coherent components of a radiation field, overcomes the shortcomings of a conventional laser source when applied to ranging. It relies on a measurement of frequency, which is inherently more accurate than measurements of response amplitudes. As will be explained, the FSF laser with phase modulation greatly improves the signal-to-noise ratio.

1.1. Basic Michelson interferometer

The schematic diagram of Fig. 1 shows the essentials of a Michelson interferometer: from a source of collimated radiation two paths, whose lengths differ by L, recombine at a detector that produces a signal proportional to the power, i.e. proportional to the square of the local electric field. The two contributions to the detected field are derived from a common source field but differ by the delay time $T \equiv 2L/c$. Thus the detector signal has the form

$$S(t,T) = \mathscr{N}\{|E(t)|^2 + |E(t-T)|^2 + 2Re[E(t)E(t-T)^*]\}. \quad (1)$$

Here, the factor $\mathscr{N}$ expresses the efficiency of the detectionprocess as related to the square of the electric field. Note that when the material of the target differs from that of the reference there occurs upon reflection a difference in phase that acts as an increment of length [14]; we here ignore this phase difference.

* Corresponding author. Tel.: +1 925 455 0627.
E-mail address: bwshore@alum.mit.edu (B.W. Shore).

0030-4018/$ - see front matter © 2009 Elsevier B.V. All rights reserved.
doi:10.1016/j.optcom.2009.02.042

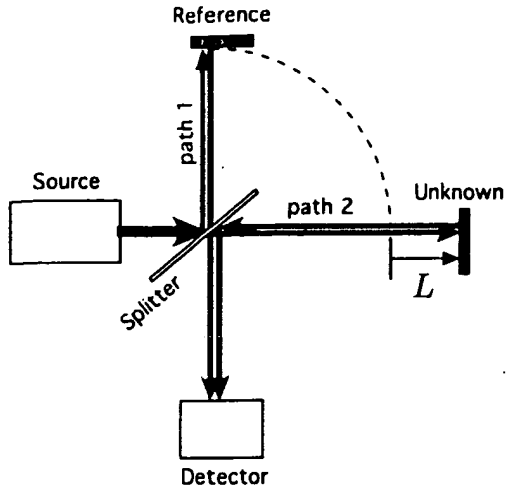

Fig. 1. Basic schematic layout of a Michelson interferometer, showing light source, power detector, and two arms. For clarity the overlapping beams are shown here as slightly offset spatially.

The simplest implementation of such a Michelson interferometer occurs when the source is monochromatic, of wavelength $\lambda = 2\pi c/\omega$. We write this field, at the position of the detector, in the complex form

$$E(t) = \mathscr{E}\exp[-i\omega t]. \tag{2}$$

Here, $\mathscr{E}$ is the amplitude of the source field and ω its frequency. It is this field that, after passing through the two paths of the interferometer, appears at the detector to produce a signal.

With such a field the detector signal is independent of time t and is expressible as

$$S(t,T) = \mathscr{G}[1+\cos(\omega T)], \tag{3}$$

where $\omega T = 4\pi L/\lambda$. The constant $\mathscr{G} = 2|\mathscr{E}|^2\mathscr{N}$ determines the size of the signal for a given electric field. Measurements of this signal, for varying optical frequency ω, provide values of $\cos(\omega T)$ and with that a measure of the ratio L/λ. Thus the technique is capable of providing values of L with an accuracy better than the optical wavelength λ, but with an ambiguity (of λ) arising from the periodicity of the cosine. When used for measurements of distance a classical interferometers cannot give values of absolute distance, only distances relative to some integer multiple of the wavelength. There are many methods capable of resolving this ambiguity [15–17]. One of them uses a phase-modulated light source. The following paragraphs review the operation of that technique, as a preliminary to the discussion of phase modulation in FSF lasers.

1.2. Absolute distance measurements using a phase-modulated light source

One of the suggestions for making absolute measurements of distance using an interferometer came from Webb et al. [18], who suggested the use of a phase-modulated laser as interferometer input. We here follow their approach and consider a light source upon which we impose a specified phase variation $\varphi(t)$,

$$E(t) = \mathscr{E}\exp[-i\omega t - i\varphi(t)]. \tag{4}$$

The detector signal is then expressible as

$$S(t,T) = \mathscr{G}\{1+\cos[\omega T + \varphi(t) - \varphi(t-T)]\}. \tag{5}$$

A particularly useful phase variation is a sinusoidal modulation, achievable using an electro-optical modulator driven at a radio frequency Ω

$$\varphi(t) = \varphi_0 + \beta\sin(\Omega t + \vartheta). \tag{6}$$

Here, β is the modulation index, φ_0 is the initial optical phase and ϑ is the initial phase of the modulation signal.

For such harmonic modulation of the phase $\varphi(t)$ the phase difference $\varphi(t) - \varphi(t-T)$ is also sinusoidal

$$\begin{aligned}\varphi(t) - \varphi(t-T) &= \beta\{\sin[\Omega t + \vartheta) - \sin(\Omega(t-T) + \vartheta]\}\\ &= 2\beta\sin(\Omega T/2)\cos[\Omega(t - T/2) + \vartheta]\\ &\equiv z\sin(\Omega t + \phi),\end{aligned} \tag{7}$$

with the amplitude and phase

$$z = 2\beta\sin(\Omega T/2), \quad \phi = \vartheta - (\Omega T + \pi)/2. \tag{8}$$

The resulting interferometer signal is

$$\begin{aligned}S(t,T) &= \mathscr{G}\{1+\cos[\omega T + z\sin(\Omega t + \phi)]\}\\ &\equiv \mathscr{G}\{1+\cos(\omega T)\cos[z\sin(\Omega t+\phi)]\\ &\quad - \sin(\omega T)\sin[z\sin(\Omega t+\phi)]\}.\end{aligned} \tag{9}$$

By using the Jacobi–Anger identities

$$\sin(z\sin\chi) = 2\sum_{k=1}^{\infty} J_{2k-1}(z)\sin[(2k-1)\chi], \tag{10}$$

$$\cos(z\sin\chi) = J_0(z) + 2\sum_{k=1}^{\infty} J_{2k}(z)\sin(2k\chi), \tag{11}$$

we rewrite the signal as [18]

$$\begin{aligned}S(t,T) = \mathscr{G}\Bigg\{&1 + \cos(\omega T)J_0(z) + 2\cos(\omega T)\sum_{k=1}^{\infty} J_{2k}(z)\sin[2k\Omega t + 2k\phi]]\\ &-2\sin(\omega T)\sum_{k=1}^{\infty} J_{2k-1}(z)\sin[(2k-1)\Omega t + (2k-1)\phi]\Bigg\}.\end{aligned} \tag{12}$$

The signal of Eq. (12) is a superposition of the harmonics of the modulation frequency Ω, each weighted by an appropriate Bessel function. Viewed in the frequency domain these appear as discrete components. We can use a narrow-band filter to select any individual harmonic, using phase-locked detection or other means. In this way we can restrict consideration to a single value of k.

For example, consider a filter that selects just the first-harmonic, $k = 1$. The signal responsible for this harmonic is

$$\begin{aligned}S_1(t,T) &= -2\mathscr{G}J_1(z)\sin(\omega T)\sin(\Omega t + \phi)\\ &\equiv \mathscr{G}J_1(z)[\cos(\Omega t + \phi + \omega T) - \cos(\Omega t + \phi - \omega T)].\end{aligned} \tag{13}$$

From the measured amplitude of this signal we obtain the value of a Bessel function $J_1(z)$. This gives information about z, from which we obtain information about the absolute value of the delay T. Because the modulation frequency Ω is radiofrequency (RF), it has a wavelength that is orders of magnitude longer than the optical wavelength of the light source. It is this long wavelength, rather than the optical wavelength, that determines the ambiguity with which we measure the distance L.

This method of ranging has two drawbacks. First, we have to adjust the interferometer to maximize $\sin(\omega T)$ in Eq. (13). Second, the method relies on a quantitative measurement of light intensity. From the magnitude of the signal we obtain the argument of the Bessel function z and, from Eq. (8), the time delay T. It is difficult to calibrate measurements of intensity, and hence the method has intrinsically low accuracy. These drawbacks have prevented practical application of the method for ranging using Michelson interferometer and phase-modulated light.

2. Optical ranging using a FSF laser

The development of frequency shifted feedback (FSF) lasers [1–13] offers a means of overcoming the previous limitations of

RF-modulated interferometry and of obtaining very high accuracy. The basic principles underlying a FSF laser are readily understood: it comprises an optical cavity (or closed loop) in which there occurs a frequency-shifting element, typically an acousto-optic modulator (AOM), and material that provides gain to a range of frequencies. A small portion of the cavity radiation emerges as output; see Fig. 2.

From a single seed field of frequency ω_s and phase $\varphi_s(t)$ a succession of round trips within the bounded laser cavity (or fiber loop) produce a set of frequencies, spaced equidistantly by the frequency shift Δ induced by the AOM. Typically the gain bandwidth is sufficient to amplify a large number (>10^4) of discrete frequency components, each with definite frequency and phase. These form a frequency comb spaced by the AOM frequency Δ.

As we explain below, instead of one laser field an FSF laser provides a large number of field components, each of which gives a similar contribution to the first-harmonic signal, but with different phases. One might expect that the averaging of so many signals would eliminate any interference effects. On the contrary, we will show that, when the modulation frequency matches a delay-dependent value, the signal is greatly enhanced; from a measurement of this frequency one obtains a very accurate value of the delay T and hence of the distance.

2.1. The FSF laser

The output field from a FSF laser is the sum of many components

$$E(t) = \sum_n \mathscr{E}_n \exp[-i(\omega_s + n\Delta)t - i\Phi_n - i\varphi_s(t - n\tau)], \tag{14}$$

Component n has a fixed frequency that has been shifted from ω_s by $n\Delta$. It has the phase of the seed laser taken at an early time $\varphi_s(t - n\tau)$ and it has undergone an additional phase shift,

$$\Phi_n = n\tau[\omega_s + (n+1)\Delta/2]. \tag{15}$$

where τ is the round-trip time within the FSF cavity. Gain from the amplifying medium and loss from the filter alter the original seed amplitude $\mathscr{E}_0$ to the value $\mathscr{E}_n$. As earlier work has shown [5], the distribution of amplitudes is well described by a Gaussian centered at a peak value n_{max} and of width n_W. In this approximation the amplitude $\mathscr{E}_n$ is

$$\mathscr{E}_n = \mathscr{E}_0 \exp\left[-\frac{(n - n_{max})^2}{n_W^2}\right]. \tag{16}$$

Fig. 3 illustrates the distribution of field components, showing the varying amplitudes, spaced by the AOM frequency Δ. The figure shows a representative distribution of gain and of loss from the filter. The peak of the Gaussian, parametrized by n_{max}, occurs close to the frequency at which gain equals loss.

2.2. Coherence properties of the FSF laser output

It is well known that the output of a multimode laser can, when the modes are phase-locked, appear as a periodic succession of very short pulses [19]. The frequencies contributing to this output are separated by the free spectral range (FSR) of the laser cavity, $2\pi/\tau$ for a round-trip time of τ, and their phases vary linearly with frequency. A FSF laser can also operate in a regime in which the output is a train of short pulses [20]. The field is then a set of mode-locked frequencies spaced by the FSR, $2\pi/\tau$.

However, for use in optical ranging, the operating regime of the FSF laser is such that no mode-locking occurs. The frequencies of the output field, are spaced by the AOM frequency Δ, and their static phases Φ_n vary quadratically with component number n. The temporal output is periodic with the period $2\pi/\Delta$ and appears as a train of frequency-chirped pulses [5].

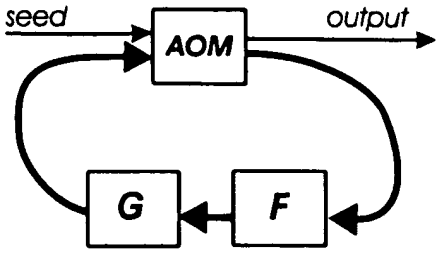

Fig. 2. Symbolic diagram of a ring cavity showing gain G, spectral filter F and frequency-shifter AOM, as well as seed and output (from [7]).

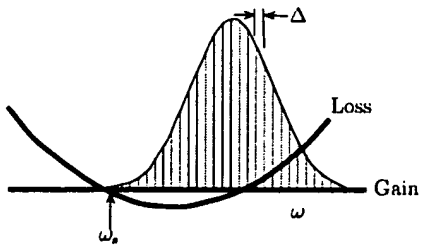

Fig. 3. Frequency components of FSF laser, spaced by Δ, as a function of frequency ω. Gain and filter loss are shown, as is the seed frequency ω_s.

2.3. Optical ranging using a FSF seed having sinusoidally modulated phase

The extension of the discussion of a single phase-modulated laser to a FSF laser is straightforward. Let us assume that the phase of the FSF seed laser is modulated as

$$\varphi = \beta \sin(\Omega t + \vartheta). \tag{17}$$

When such phase modulation of the seed is present the phase of a specific FSF component n reads

$$\varphi_n = \beta \sin(\Omega(t - n\tau) + \vartheta). \tag{18}$$

Therefore, we have

$$\varphi_n = \beta \sin(\Omega t + \vartheta_n), \quad \vartheta_n = \vartheta - n\Omega\tau, \tag{19}$$

meaning that each FSF component has, in addition to the static phase Φ_n, a modulated phase φ_n that originates with the seed-laser phase. The initial phase of that modulation varies linearly with component number n.

Eq. (12) has given the expression for the signal for a single modulated laser. With the FSF laser we have many such modulated components. The detector signal sums the results from each of them, appropriately phased.

For example, consider filtering that selects just the modulation frequency Ω (the first of the harmonics). Then the signal, generalizing Eq. (13), is the sum of all the individual components of the FSF field,

$$S_1(t,T) = 2\mathscr{N} J_1(z) \sum_n |\mathscr{E}_n|^2 \{\cos(\Omega t + \phi_n + [\omega_s + n\Delta]T) - \cos(\Omega t + \phi_n - [\omega_s + n\Delta]T)\}, \tag{20}$$

where

$$\phi_n \equiv \vartheta_n - (\Omega T + \pi)/2, \quad \vartheta_n = \vartheta - n\Omega\tau. \tag{21}$$

We rewrite this as two separate sums

$$S_1(t,T) = 2\mathscr{N} J_1(z) \sum_n |\mathscr{E}_n|^2 \cos[\Omega t - n(\Omega\tau - T\Delta) + \psi_+] - 2\mathscr{N} J_1(z) \sum_n |\mathscr{E}_n|^2 \cos[\Omega t - n(\Omega\tau + T\Delta) + \psi_-], \tag{22}$$

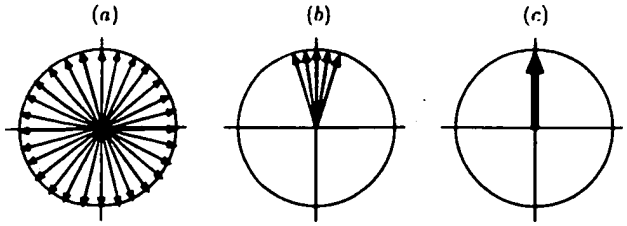

Fig. 4. Schematic distribution of vector phases. (a) a uniform distribution of vectors resulting from small constant phase increments between components of the radiation field. (b) A narrow distribution of phases, as occurs when the resonance condition is nearly but not exactly fulfilled. (c) All vectors have phases that obey the resonance condition.

where

$$\psi_{\pm} \equiv \pm\omega_s T - (\Omega T + \pi)/2 + \vartheta. \tag{23}$$

Each of these sums is responsible for a distinct resonance (an enhancement of the signal within a narrow frequency range) as noted in the following paragraphs.

2.4. Vector picture of interferometer output signal

Because the terms of the summation have amplitude and phase, they can be regarded as vectors. When the modulation frequency Ω obeys the resonance condition

$$\Omega\tau = \pm T\Delta + m2\pi, \quad m = 0, 1, 2, \ldots. \tag{24}$$

then all vectors in one of the sets are aligned in the same direction. The resulting vector has, as magnitude, the arithmetic sum of the amplitude of each of the many components. The resulting first-harmonic signal is

$$S_1(t,T) = \pm 2\mathcal{N} J_1(z) \sum_n |\mathscr{E}_n|^2. \tag{25}$$

Fig. 4c illustrates this situation. By contrast with the results of a single laser, here we have the sum of many components (typically $>10^4$), and so the signal is greatly enhanced by comparison with a single laser.

However, when the modulation frequency is nonresonant, so that the argument $(\Omega\tau \pm T\Delta)$ is nonzero, the vectors point, with angular increment $n(\Omega\tau \pm T\Delta)$, into different directions. Their summed amplitude will therefore typically be small, or zero. Fig. 4a illustrates this situation.

To evaluate the interferometer-arm delay T, from which we derive the ranging information, we must evaluate the modulation frequency Ω for which the resonance condition of Eq. (24) holds. This is recognizable as the modulation frequency which maximizes the interferometer output signal at a frequency

$$\Omega_m^{(\pm)} = \pm\frac{\Delta}{\tau}T + m\frac{2\pi}{\tau}. \tag{26}$$

The components will be in phase, and the signal will be large, only within a small interval

$$\delta\Omega \sim \frac{2\pi}{n_W}\frac{T}{\tau}\Delta. \tag{27}$$

of frequencies near such a resonance frequency, set by the width n_W of the component distribution, see Eq. (16). Fig. 4b illustrates this situation.

Our optical ranging procedure, using a phase-modulated seed for a FSF laser, is based upon identifying the frequency where the resonance occurs. We do not need to measure relative intensity and interpret this through a Bessel function. It is this change, from measuring relative intensity to measuring a frequency (facilitated by strong signal enhancement at resonance), that gives our method such an advantage.

Our procedure also dramatically enhances the signal observed with an unseeded FSF laser [8,9]. The phases of a FSF laser seeded by a phase-modulated input laser have well defined phases. By contrast, when the FSF grows from spontaneous emission the FSF field comprises a continuous distribution of frequency combs. Within any comb the phases are fixed by geometry, and are not adjustable, but the phases between different combs (started by spontaneous emission) are random. Our method uses the coherence of the various components to enhance the signal compared with growth from noise.

2.5. Observing higher harmonics

We remark that the resonances exist in the amplitudes of all harmonics of the output of Michelson interferometer excited by FSF laser with phase-modulated seed laser. For example, the signal of the second harmonic is

$$S_2(t,T) = 2\mathcal{N} J_2(z) \sum_n |\mathscr{E}_n|^2 \sin[2\Omega t - n(2\Omega\tau - T\Delta) + \psi_+^{(2)}] - 2\mathcal{N} J_2(z) \sum_n |\mathscr{E}_n|^2 \sin[2\Omega t - n(2\Omega\tau + T\Delta) + \psi_-^{(2)}], \tag{28}$$

where

$$\psi_{\pm} \equiv \pm\omega_s T - (2\Omega T + \pi)/2 + 2\vartheta. \tag{29}$$

The resonance condition is

$$\Omega\tau = \frac{1}{2}[T\Delta + 2\pi m]. \tag{30}$$

In a similar way one can show that for the kth harmonic the resonance condition is

$$\Omega\tau = \frac{1}{k}[T\Delta + 2\pi m]. \tag{31}$$

Each harmonic signal varies in proportion to a Bessel function whose argument z, defined in Eq. (8), varies with distance L. When a distance is such that the Bessel function $J_1(z)$ for order 1 is small, thereby limiting the signal strength, the Bessel function $J_k(z)$ of a higher order will then give a larger signal.

3. Summary and outlook

Phase modulation interferometry has been earlier suggested and is well understood [18]. The physics of FSF laser operation is equally well understood [5]. The concept of ranging with a free-running FSF laser has been described and demonstrated some years ago by Japanese researchers [8,9]. However, the free-running FSF laser is not a practical device for industrial applications.

The use of a phase-modulated FSF seed overcomes the drawbacks noted for a free-running FSF laser. As has been demonstrated, this technique provides dramatic enhancement of the interferometer output signal by orders of magnitude if, and only if, the modulation frequency Ω obeys the resonance condition of Eq. (24). The accuracy of the ranging technique stems from the accuracy with which frequency measurements can be made, in contrast to measurements of relative intensity.

Although the literature contains rigorous mathematical treatments of FSF lasers [10] the present discussion offers a simple straightforward picture of the physics behind the observation of the dramatic signal enhancement resulting from the phase modulation of the FSF seed.

Acknowledgements

We acknowledge support from the Stiftung Rheinland-Pfalz für Innovation and the Research Center OPTIMAS at the Technisches Universität Kaiserslautern.

References

[1] P.D. Hale, F.V. Kowalski, IEEE J. Quant. Electron. 26 (1990) 1845.
[2] K. Shimizu, T. Horiguchi, Y. Koyamada, Exp. Appl. Opt. 32 (1993) 6718.
[3] F.V. Kowalski, S. Balle, I.C.M. Littler, K. Bergmann, Opt. Eng. 33 (1994) 1146.
[4] K. Nakamura, F. Abe, K. Kasahara, T. Hara, M. Sato, H. Ito, IEEE J. Quant. Electron. 33 (1997) 103.
[5] L. Yatsenko, B.W. Shore, K. Bergmann, Opt. Commun. 236 (2004) 183.
[6] V.V. Ogurtsov, L.P. Yatsenko, V.M. Khodakovskyy, B.W. Shore, G. Bonnet, K. Bergmann, Opt. Commun. 266 (2006) 266.
[7] L.P. Yatsenko, B.W. Shore, K. Bergmann, Opt. Commun. (2008). doi:10.1016/j.optcom.2008.10.002.
[8] K. Nakamura, T. Miyahara, H. Ito, Appl. Phys. Lett. 72 (1998) 2631.
[9] K. Nakamura, T. Hara, M. Yoshida, T. Miyahara, H. Ito, IEEE J. Quant. Electron. 36 (2000) 305.
[10] L.P. Yatsenko, B.W. Shore, K. Bergmann, Laser Opt. Commun. 242 (2004) 581.
[11] V.V. Ogurtsov, L.P. Yatsenko, V.M. Khodakovskyy, B.W. Shore, G. Bonnet, K. Bergmann, Opt. Commun. 266 (2006) 627.
[12] K.A. Shore, D.M. Kane, IEEE Procc-Optoelectron. 153 (2006) 284.
[13] V.V. Ogurtsov, V.M. Khodakovskyy, L.P. Yatsenko, B.W. Shore, G. Bonnet, K. Bergmann, Opt. Commun. 281 (2008) 1679.
[14] L.P. Yatsenko, M. Loeffler, B.W. Shore, K. Bergmann, Appl. Opt. 43 (2004) 3241.
[15] P. de Groot, Appl. Opt. 30 (1991) 3612.
[16] P. de Groot, J. McGarvey, Opt. Lett. 17 (1992) 1626.
[17] B. Chen, X. Cheng, D. Li, Appl. Opt. 41 (2002) 5933.
[18] D.J. Webb, R.M. Taylor, J.D.C. Jones, D.A. Jackson, Opt. Commun. 66 (1988) 245.
[19] L. Dahlstrom, Opt. Commun. 5 (1972) 157.
[20] G. Bonnet, S. Balle, T. Kraft, K. Bergmann, Opt. Commun. 123 (1996) 790.